Journal of Rock Mechanics and Geotechnical Engineering 14 (2022) 616–624

Contents lists available at ScienceDirect

Journal of Rock Mechanics and Geotechnical Engineering

journal homepage: www.jrmge.cn

Full Length Article

Visualization and quantification of soil laboratory impact compaction

Wei Hu [a], Pawel Polaczyk [a], Hongren Gong [b], Yuetan Ma [a], Baoshan Huang [a,*]

[a] Department of Civil and Environmental Engineering, University of Tennessee, Knoxville, 851 Neyland Dr, Knoxville, TN, 37996, USA
[b] Key Laboratory of Road and Traffic Engineering of Ministry of Education, Tongji University, Shanghai, 201804, China

ARTICLE INFO

Article history:
Received 11 December 2020
Received in revised form
22 May 2021
Accepted 17 July 2021
Available online 2 August 2021

Keywords:
Impact compaction
Soil compaction
Locking point
Accelerometer
Dynamic response

ABSTRACT

As important methods to guide the field soil compaction, the standard and modified Proctor tests for laboratory compaction have remained unchanged for decades, which should be improved to better understand the compaction process and the properties of soils. In this study, an accelerometer was installed on a Marshall impact compactor to capture the dynamic response of three types of soils during compaction. The experimental test results indicated that the acceleration curve for each blow gradually evolved to a stable pattern following the progress of compaction, and the impact and gyratory locking points were linearly related with coefficient of determination R^2 equal to 0.59. The impact compaction curve could be further constructed by filtering the structural resonance, which can be used to quantify the compactability of soil materials. Although each type of soil had a unique set of compaction curves, the slope and value of compaction curve altered accordingly as the moisture content changed for the same soil. In addition, the average acceleration value at the final compaction stage could serve as the target value of soil stiffness.

1. Introduction

As the most common and important material encountered in infrastructure system, soil serves as an engineering medium for construction of roadbeds, foundations, dams, and buildings. Before it can be used for such applications, a vital part of the construction process is soil compaction to improve its engineering properties, such as stiffness, compressibility, and permeability (Cetin et al., 2007; Caicedo et al., 2014). To achieve this, there are several compaction methods which can be classified as static, impact, vibrating, gyrating, rolling, and kneading (Ito and Komine, 2008; Feng et al., 2013; Vukadin, 2013). Different compaction techniques may be suitable for different soil types. The vibrating compaction is more applied in sands and gravels to cause re-orientation of the soil particles, whereas a sheepsfoot roller could be used in silts and clays to drive air out of the soil (Das and Sobhan, 2013).

However, regardless of the type of soil, the most commonly and currently used laboratory tests for soil compaction, the standard and modified Proctor tests, can be explicitly classified as impact compaction, since both tests are performed by dropping a large mass onto the surface of the soil (Virgil Ping et al., 2002). These tests offer the maximum dry density and the optimum moisture content of the tested soil to guide the field compaction, but without the ability to offer additional information such as the compactibility of soil. As a similar engineering material, the laboratory compaction of asphalt has undergone a conversion from the impact compaction to the gyratory compaction. The traditional Marshall compaction for asphalt mixture is similar to the standard and modified Proctor tests utilizing the same impact method, which was gradually replaced by the Superpave gyratory compactor with the ability to apply a vertical load and a self-adjusting kneading action simultaneously (Khan et al., 1998). One key advantage of gyratory compactor lies in that it can monitor the specimen height after each gyration, thus a densification curve can be obtained to evaluate the compactability of asphalt materials (Jia et al., 2019). Attributed to this advantage, Anderson et al. (2002) utilized the slope of densification curve to describe compactability with a higher slope indicating higher resistance to compaction. Another concept used to evaluate compactability is the locking point, which defines a threshold on the densification curve, and beyond that further densification seems impossible (Vavrick et al., 2002; Mohammad and Al-Shamsi, 2007).

Similarly, the concepts of densification curve and locking point can benefit the soil compaction by indicating the effort needed for the field compaction, and benefit the laboratory impact compaction

* Corresponding author.
E-mail address: bhuang@utk.edu (B. Huang).
Peer review under responsibility of Institute of Rock and Soil Mechanics, Chinese Academy of Sciences.

https://doi.org/10.1016/j.jrmge.2021.07.001

by offering more useful information. A potential approach to achieve this is the utilization of accelerometer. For example, at the initial development of Clegg impact tester, a standard Proctor-type hammer was equipped with an accelerometer and utilized to measure the deceleration of the falling hammer mass (Clegg, 1976). By dropping a hammer four times in the same place and identifying the highest deceleration value, it can be used to determine the hardness of compacted soil with a higher value indicating a stiffer material. Previous studies revealed that it can be correlated well with a California bearing ratio (CBR) value (Clegg, 1979). However, the design of the Proctor hammer and its compaction process make the Proctor compactor not the ideal candidate for accelerometer installation. The Proctor hammer has a cylindrical outer sleeve, and the impact force is applied manually on different locations of specimens, making the installation of accelerometer and construction of densification curve challenging. As a comparison, the Marshall compactor can apply the impact force automatically on the whole surface of specimen, and an accelerometer can be easily placed on the falling mass. There have been several attempts to utilize accelerometers on Marshall compactor as a calibration method for the Marshall hammer (Siddiqui et al., 1988; Shenton et al., 1994; Sebesta et al., 2008). It was found that the high level of noise in the signal from the accelerometer impaired the ability for calibration, which may also affect the potential of using Marshall compactor to monitor the compactibility of soil. However, recent studies overcame this difficulty by identifying the change pattern in acceleration curve during the asphalt compaction, and therefore obtained the impact locking point which correlated well with the gyratory locking point for several types of asphalt mixtures (Polaczyk et al., 2018, 2019a, b). Based on the previous studies, it is possible to adopt the Marshall compactor as an alternative to the Proctor compactor to capture the change of soil dynamic properties using accelerometers.

The objective of this study is to evaluate the feasibility of quantifying the laboratory impact compacting process for soil materials by utilizing dynamic-based methods. To achieve this goal, a treated limestone aggregate and two types of soils which commonly serve as paving materials were utilized, and the change of this dynamic soil-impact compactor system during the compaction was monitored by using an accelerometer. The Proctor test and Superpave gyratory compaction were also performed to obtain soil volumetric properties.

2. Materials and test methods

2.1. Materials

The selected soil materials in this study include two types of subgrade soil and a treated limestone aggregate collected from paving and construction projects in Tennessee, USA. Based on the American Association of State Highway and Transportation Officials (AASHTO) classification system, the treated limestone aggregate was classified as A-1, which contained 80% of aggregate and 20% of fly ash. The first type of clayey soil (Soil 1) was classified as A-6 with a liquid limit (*LL*) of 35%, a plastic index (*PI*) of 14%, and a group index (*GI*) of 3, whereas the second type of clayey soil (Soil 2) was classified as A-7-6 with an *LL* of 42%, a *PI* of 15%, and a *GI* of 10. Fig. 1 shows the gradation of the treated limestone aggregate and soils.

2.2. Test methods

The standard Proctor test was performed to obtain the moisture content and dry density curves of the soil materials. Then by using the same moisture contents, the soil specimens were compacted by a Marshall compactor with a total of 100 blows of impact

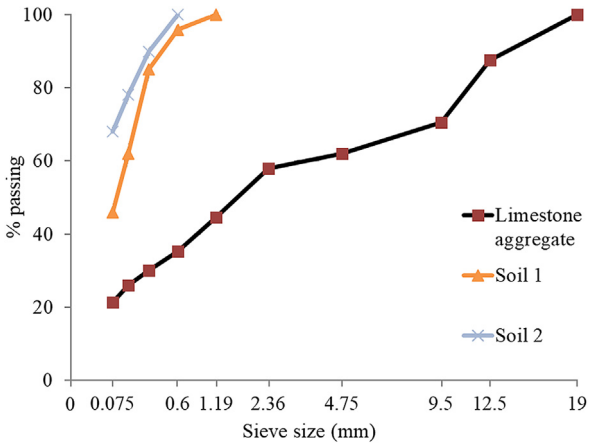

Fig. 1. Gradation of the treated limestone aggregate and soils.

compaction in a 100 mm diameter mold. The mass of Marshall specimen was 1200 g for aggregate and 800–950 g for clayey soils. In addition, the soil specimens in a 150 mm diameter mold were compacted by a Pine Instrument company AFGC125X Superpave gyratory compactor. The gyratory compaction was performed with a rate of 30 gyrations per minute, a confining pressure of 600 kPa, an angle of gyration of 1.25°, and a total number of 150 gyrations. The mass of gyratory specimen was 4500 g for the aggregate and 3000 g for clayey soils.

The Marshall compactor adopted in this study is a Humboldt Marshall mechanical compactor. With a 4.536 kg compaction hammer dropped from a height of 457.2 mm, the Marshall hammer offers a heavier impactive effort than the standard Proctor hammer, which has a 2.5 kg hammer and a drop height of 305 mm. It should be noted that the modified Proctor method uses the same 4.536 kg hammer with the same 457 mm drop height as the Marshall compactor. To monitor the dynamic responses from impacting, a PCB Piezotronics 5000*g* ($1g = 9.81\ m/s^2$) accelerometer was installed on the compaction hammer, as shown in Fig. 2. The accelerometer was connected to the National Instrument data acquisition system with a sampling rate of 10,000 Hz, and a LabVIEW system design software was used to record the acceleration data.

3. Test results

3.1. Moisture-density curves from impact and gyratory compaction

Fig. 3 illustrates the relationship between dry density and moisture content from the impact and gyratory compaction for different soils. Since the gyratory compactor could offer the highest compactive effort, the specimens achieved the highest dry density for the same soil at the same moisture content compared to the impact tests. For the clayey soils, the gyratory compactor specimens also showed a lower optimum moisture content compared to the impact tests due to the difference in applied energies. As similar impact methods, the moisture-dry density curves from the Marshall compactor shared similar patterns and values compared to that from the Proctor test for the same soil. The optimum moisture content determined by both impact tests was 7.5% for the limestone aggregate, 23% for clayey soil 1, and 28% for clayey soil 2. The difference between the maximum dry density from two impact tests was 0.12 g/cm^3 for the limestone aggregate, 0.09 g/cm^3 for clayey soil 1, and 0.05 g/cm^3 for clayey soil 2. Based on the results, it could be concluded that the Marshall compactor can serve as an

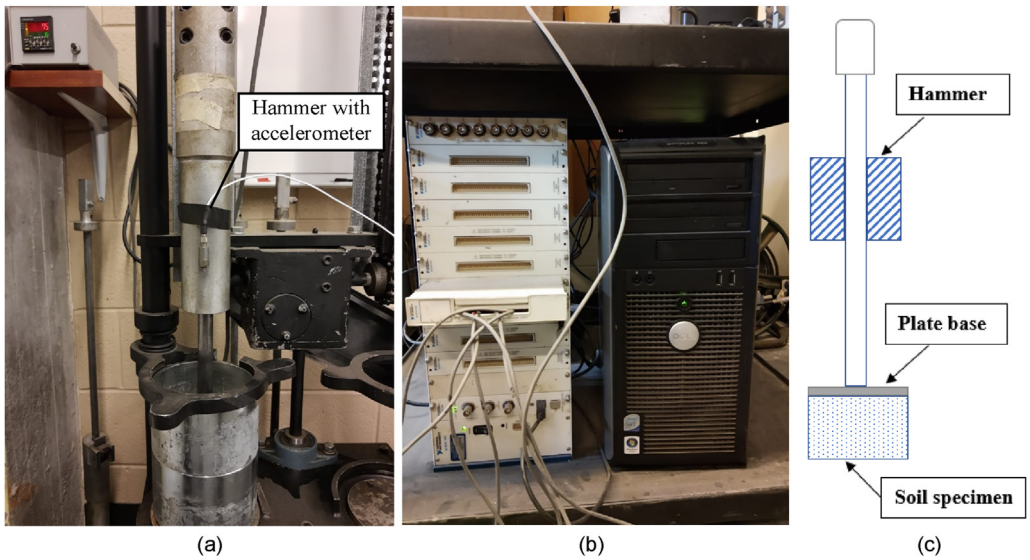

Fig. 2. The impact hammer with an accelerometer: (a) The Marshall compactor, (b) The data acquisition system, and (c) Hammer diagram.

alternative for the Proctor test to demonstrate the impact compacting process for soil materials.

It should be noted that the 10% moisture content specimen for the limestone aggregate was not prepared for the gyratory compaction due to moisture extrusion. During the compaction process, the moisture content may change from the initial targeted value to the lower final as-compacted value, especially for the gyratory compaction. Despite this, the targeted value of moisture contents was utilized for the dry density-moisture content curve construction.

3.2. Impact locking point

After the Marshall compaction, the acceleration data from the high-*g* accelerometer were collected and analyzed. The interval between two consecutive hammer impacts was around 0.975 s, whereas a duration of one impact was about 0.05 s. To illustrate the dynamic pattern during the compaction, the acceleration curves for the first blow, the 20th blow, and the 80th blow for each soil at its lowest moisture content are presented in Fig. 4.

Fig. 4 presents the tendency of acceleration curves during the compaction. For each blow, there will be a main acceleration pulse after the initial impact. As shown in Fig. 2, the Marshall hammer drops on a steel plate instead of the specimen surface, which arouse resonance or noise. Therefore, the main pulse was followed by oscillations of a much higher frequency, which kept the same pattern for the same specimen but varies among different materials. When focusing on the main pulse, it changed from a fluctuation among positive and negative peaks at the initial stage as shown in Fig. 4a, d and g, since the specimen was compressed significantly at this time, then to a stable pattern with one or two main peaks as shown in Fig. 4c, f and i following the progress of compaction, since the specimen became incompressible and stable. For all the soil materials and all the moisture contents, eventually the acceleration main pulse would reach a stable pattern at a certain blow number, after that the acceleration curves were similar without significant changes. It is reasonable to assume that as the density of the soil material increases, the stiffness of soil also increases causing changes in the acceleration response. At a certain point, the density and stiffness of soil cannot be further increased, indicated by the stable pattern of acceleration curve. Similar to the gyratory locking point which is defined as a threshold on the densification curve beyond which the mix structure starts to resist further compaction and aggregates can be fractured, the blow number upon which the acceleration curve reaches the stable pattern could be defined as the impact locking point. To accelerate the identification of locking point, the trendline of five-period moving average was utilized to smooth the acceleration curve. Fig. 5 shows the five-period moving average trendline for the first and the last five blows for the aggregate with 5% moisture content. The data between two consecutive blows were deleted so as to accommodate five blows into one figure. It could be observed that the trendline evolved from multiple peaks to a stable single peak. Based on this, the impact locking point was decided as the first blow when the trendline evolved to a stable single peak. Fig. 6 shows the relationship between impact and gyratory locking point based on five-period moving average trendline. For the gyratory compaction, the locking point of soil materials is determined as the first gyration of three consecutive gyrations at the same height (Vavrik and Carpenter, 1998).

It can be observed that the locking points from different compaction methods share a similar trend. For all the soil materials included in this study, both the impact and gyratory locking point decreased with the increase of moisture content, indicating that less compaction effort was needed for the material to reach its stable compaction stage at high moisture content. However, unlike the gyratory locking point which could be easily identified from the height record, the identification of impact locking point was not easy since there were no clear transitions in acceleration curves for some specimens.

3.3. Compaction curve construction for impact compaction

Unlike the conventional Marshall compaction, one advantage of the gyratory compaction lies in its densification curve through which the compactability of soil can be visually identified. By adopting the accelerometer on the hammer, there is a potential to construct the compaction curve for the soil impact compaction. However, there are two characteristics in acceleration data for the Marshall compaction. When the interval between two blows is around 1 s, the actual acceleration peak curve for each blow could only last 0.002 s if excluding the structural resonance. Second, as

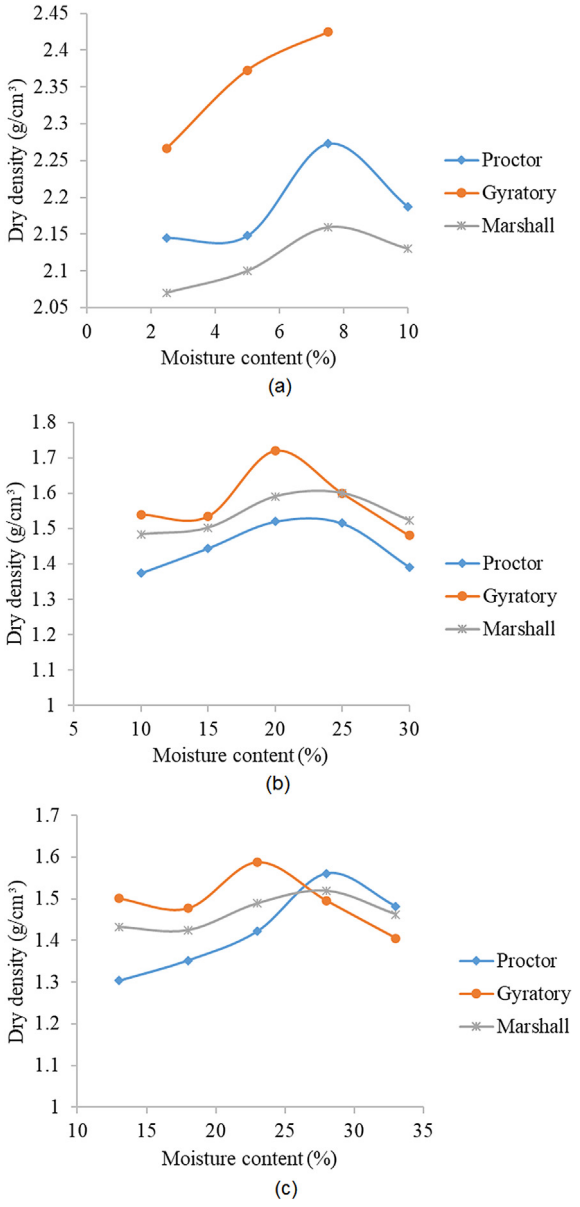

Fig. 3. Comparison of moisture content-dry density curves: (a) Limestone aggregate, (b) Soil 1, and (c) Soil 2.

shown in Figs. 2 and 4, the oscillations of a much higher frequency following the main pulse is mainly resulting from resonance of the hammer which is not indicating the soil stiffness. To build the soil compaction curve, the noise between two consecutive blows should be filtered. To achieve this, the acceleration data were cut off to include only one blow for each section, and then the data among certain range were deleted to filter the noise, for example, between 10*g* and −10*g*. After that, the peak value data for each section were averaged to obtain the average value for each blow indicating the soil stiffness at this point. Finally, a three-order polynomial trendline was built to serve as the compaction curve. Fig. 7 shows the compaction curves for the same aggregate specimen at 2.5% moisture content when various filtering range was adopted.

As shown in Fig. 7, applying ±50*g* filtering range was not efficient enough to filter the noise. The average value for each blow was small and no clear pattern could be observed. Increasing the filtering range to ±100*g* could improve the results, but the data points were relatively scattered. Using the filtering range of ±150*g* or ±200*g* could filter the noise effectively. The stiffness of specimen increased from close to 0 to a plateau after around 40 blows. A further expansion of the filtration range resulted in loss of effective peak value. Based on trial test results, the filtering range of ±200*g* was adopted to build the compaction curve for the aggregate and soil 1 specimens. As shown in Fig. 4, the structural oscillations after the peak curve is relatively small for soil 2, therefore the filtering range of ±100*g* was enough to filter the noise for soil 2 specimens. Fig. 8 compares the impact and gyratory compaction curves for three types of soils at varying moisture content.

For the impact compaction curve, the vertical axis represents the average acceleration value for each blow, indicating the stiffness of specimens, and the horizontal axis is the number of impact blows. For the gyratory compaction curve, the vertical axis represents the specific dry density of specimen, when the horizontal axis is the number of gyrations. In general, each type of soil had a unique set of compaction curves. However, a lower moisture content usually resulted in a higher acceleration value and a higher slope of compaction curves for all the types of soils. Following an increase of moisture content, less compaction effort was needed to reach the target stiffness or density of the specimens. Therefore, the impact compaction curve tended to fade into a straight line when the moisture content is high, since the highest stiffness could be achieved just after a few blows. Similar results could also be observed on gyratory compaction curves. With high moisture contents, the specimens reached the locking point swiftly and the total densification curve behaves like a flat line. For soil 2, although the highest impact compaction curve belonged to the specimen with the lowest moisture content like other soils, the rest of the impact compaction curves overlapped each other and did not change proportionally with the change of moisture content. This clayey soil was classified as A-7-6 and characterized as poor quality as subgrade materials. Due to its inferior strength, the specimen may be unstable during the compaction when the moisture content is high, and no meaningful compaction curve could be constructed. It should be noted that the stiffness and dry density are two different properties of soil. As an indicator of stiffness, the highest impact compaction curve usually corresponded to the lowest moisture content, whereas the highest gyratory compaction curve had the optimum moisture content for the same soil. As the dynamic compaction method, the dimension and weight of specimen may affect the test results with the fixed impact force for all the specimens. To investigate this, the same soil 2 specimens at 18% moisture content were compacted with different sample masses, i.e. 800 g and 900 g. Fig. 9 shows the two compaction curves based on the test results. It can be observed that they shared similar patterns, but the 800 g specimen had a higher peak value than the 900 g specimen due to the fact that its lower height resulted in a weakened damping effect.

As shown in Fig. 8, most of the specimens reached the plateau of impact compaction curve before 60 blows. If assuming that specimens reach a stable density and stiffness at the final stage of compaction, the average value of the last 40 blows was calculated as shown in Fig. 10. The limestone aggregate had the highest value of acceleration which changed significantly according to the change of moisture content, whereas the soil 2 had the lowest value of acceleration which reached its second peak at the optimum moisture content.

4. Discussion of results

The soil laboratory compaction is important since the field compaction criterion is established on it. Currently, the dry density and moisture content from the Proctor test are still used exclusively

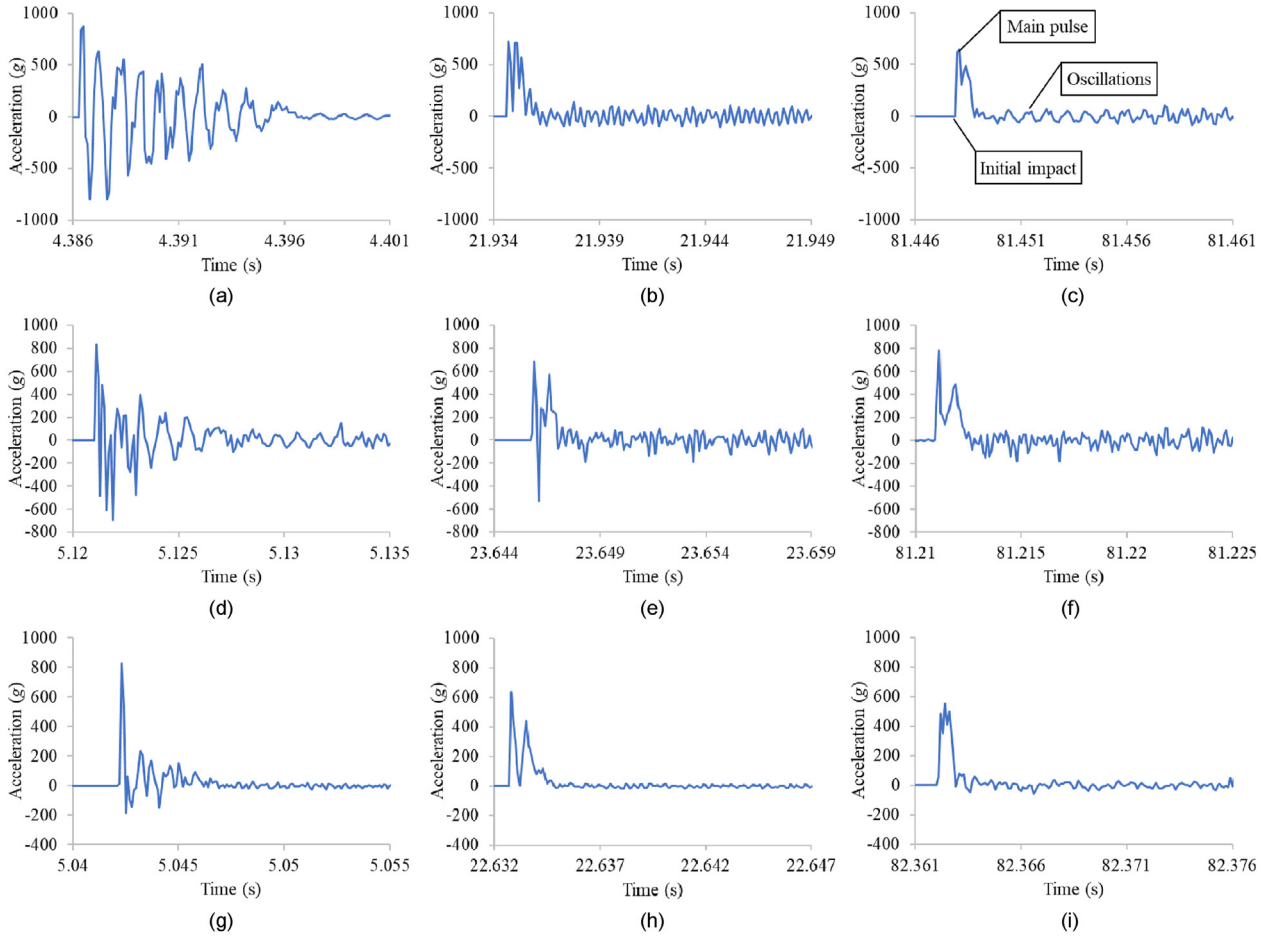

Fig. 4. Acceleration curves during the compaction: (a) Aggregate, 1st blow; (b) Aggregate, 20th blow; (c) Aggregate, 80th blow; (d) Soil 1, 1st blow; (e) Soil 1, 20th blow; (f) Soil 1, 80th blow; (g) Soil 2, 1st blow; (h) Soil 2, 20th blow; and (i) Soil 2, 80th blow.

as criteria for field compaction. However, following the development of intelligent compaction (IC) technology, a shift is occurring towards the use of soil stiffness as an alternative parameter for compaction control (Hu et al., 2017, 2018). Correspondingly, the traditional laboratory impact compaction should be evolved to monitor more soil properties as an integral part of the improved soil compaction system.

By using the high-*g* accelerometer, the impact dynamic pattern of hammer was identified from the Marshall soil compaction, which was changing constantly for each blow following the change of the property of underlying soil. Through examining the acceleration pattern for each blow, it is feasible to identify the locking point at which further impact efforts are not helpful. Although structural oscillations existed after each blow, it can be filtered so that the impact compaction curves could be built for varying moisture contents. As shown in Fig. 8, the impact compaction curve changed for both the peak value and the slope following the change of moisture content for the same material. A previous study investigated the effect of moisture content on IC soil compaction, in which the field IC compaction curves changed significantly corresponding to a change of moisture contents (Hu et al., 2020). The laboratory impact compaction curve in this study share similar trends to that study, indicating the specific compaction force needed for different moisture contents. On the other hand, a potential application of compaction curve is to evaluate the change of soil moisture content based on the change of compaction curve, which is vital for a successful field compaction.

Although soil response to high energy impact is complex, acceleration measurement of the hammer on the ground shows promise for the evaluation of soil improvement due to dynamic compaction. Chow et al. (1990) simulated the interaction of the pounder and the soil with a simple one-dimensional wave equation model, in which the soil beneath the hammer is modeled as a laterally confined elastic soil column and with only an axial mode of deformation. Despite the simplifications of the model, the calculated results were in reasonable agreement with the results from the field and laboratory. Clegg (1976) used the Clegg impact tester for evaluation of pavement base courses, which offers a desirable in situ strength evaluation for quality control purposes. Based on test results from various soil materials, he suggested that an impact value of below 400*g* would be considered “fair to poor subgrade” and above 600*g* as “good flexible base materials”. Another previous study in Indiana also evaluated the Clegg impact tester for quality control of roadway compaction and construction (Kim et al., 2010). In this study, the soil specimen was in a laterally confined mold with only axial deformation. Although the boundary conditions are not the same as in the field Clegg impact testing, the average acceleration value of the last 40 blows in the laboratory compaction as shown in Fig. 10 still reveals the different strengths among different materials and moisture contents. It is interesting to note that in general, the soil stiffness decreases while the dry density increases initially with increasing moisture content before reaching the optimum value, and the stiffness of limestone aggregate shows a more significant decline during this stage compared to the other

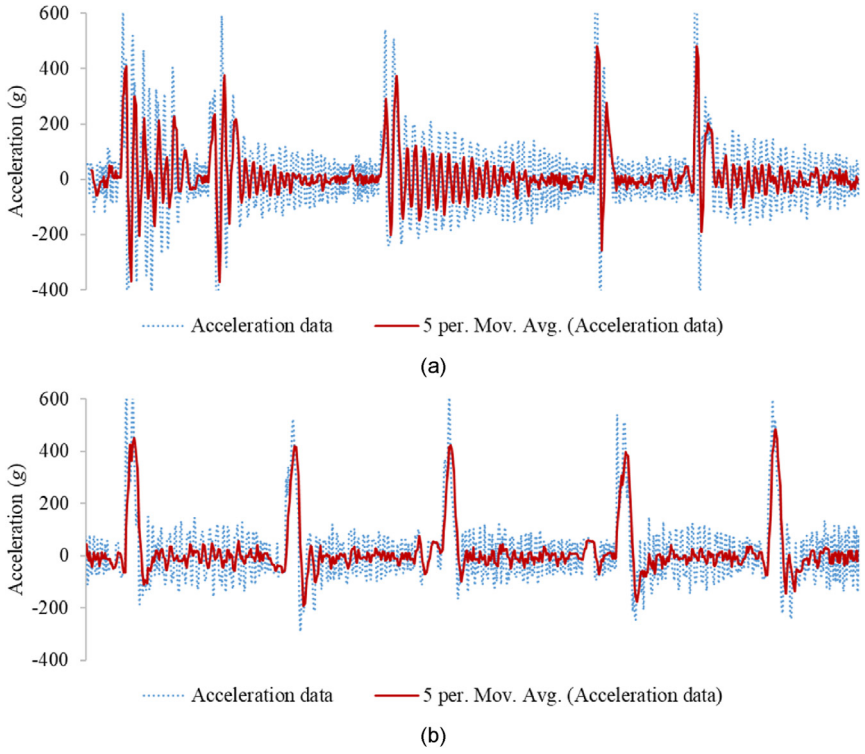

Fig. 5. The trendline of five-period moving average for aggregate with 5% moisture content: (a) The first five blows, and (b) The last five blows.

two soil materials, which demonstrates the separate contributions of matric suction versus dry density to the unsaturated soil stiffness. A previous study investigated the effect of matric suction on resilient modulus of compacted aggregate base courses (Ba et al., 2013). It was found that the limestones were more sensitive to changes in matric suction compared to the other aggregates, and resilient modulus was more correlated with matric suction than with compaction moisture content. The soil materials could be better quantified in laboratories by the average acceleration value, densification curves, locking points, and their relationships with matric suction, dry density, saturation degree, etc.

The difference between the Clegg impact tester and the Marshall compactor should be noted. The Clegg impact tester drops a hammer directly on the soil surface, whereas the Marshall hammer drops on a steel plate, not the specimen surface, which arouses more resonance or noise. Therefore, the Clegg impact tester uses the highest deceleration value to indicate the hardness of compacted soil, whereas the highest value for each blow did not show any trend for the Marshall compaction in this study. The Clegg impact tester also contains filter to remove unwanted frequencies resulting from resonance of the accelerometer and hammer.

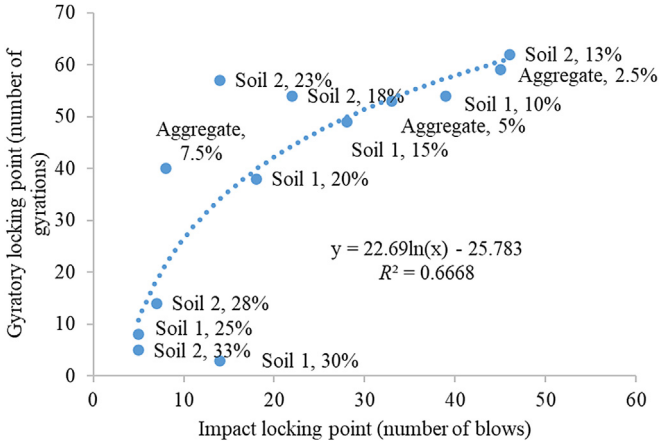

Fig. 6. Relationship between impact and gyratory locking point.

The impact test is usually performed to determine the energy absorbed or the energy required to fracture a specimen. Therefore, the cumulative input compaction energy is important. However, the absorbed energy into the specimen for each blow is complicated in this study. The hammer hits the plate base resulting in a deformation of specimen, which is neither elastic collision nor inelastic collision. To calculate the absorbed energy, the average impact force and the distance traveled after impact should be obtained. However, distance estimation is not a simple task due to this complicated impact system. Shenton et al. (1994) used a spring-mass device with force transducer for calibration of the Marshall compaction hammer. By analyzing the force time histories from multiple hammer blows, the average peak force, peak energy, cumulative energy, impulse and cumulative impulse could be determined. It is interesting to note that the typical force-time curve in that study is very similar to the acceleration-time curve in this study. The impulse is the integral of the force with respect to time. If assuming that the average acceleration is proportional to the average force and the impact duration keeps the same for each blow, the compaction curve with the average acceleration value in this study indicated the change of impulse during the compaction process.

5. Limitations

As a preliminary study, the attempt in this paper demonstrated that the potential of using accelerometer for laboratory impact compaction is promising. This study can serve as a basis for

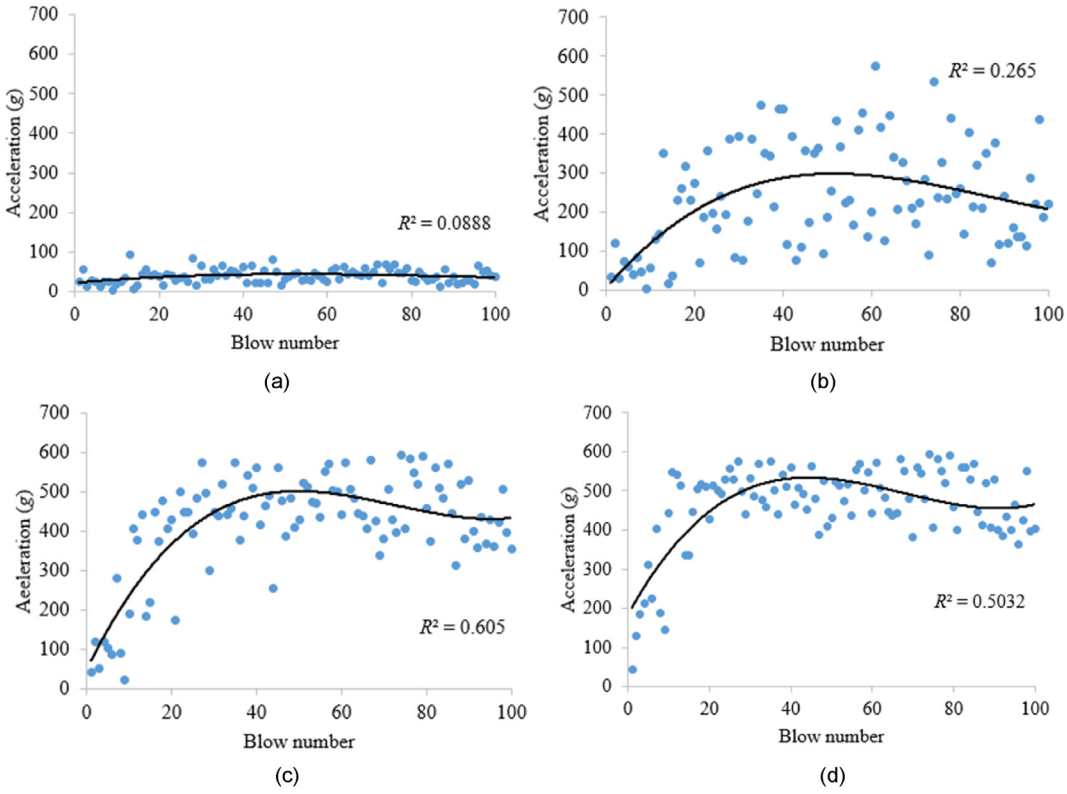

Fig. 7. Building compaction curve using various filtering range for limestone aggregate: (a) ±50*g*, (b) ±100*g*, (c) ±150*g*, and (d) ±200*g*. R^2 is the coefficient of determination.

developing a simple laboratory test to obtain the target stiffness and a "spectrogram" among stiffness, density, and moisture content for a stiffness-based soil compaction control. However, there are a few limitations which should be improved in the future. First, as a compactor designed for the asphalt compaction, the impact force of the Marshall compactor is significantly stronger than that of the Proctor test. When the specimen moisture content was low, the compaction curve pattern was easy to identify; however, when the moisture content is high, the specimen reaches its highest stiffness so fast that the compaction curve pattern is hard to discern due to this heavier impact force. Future studies should lighten the hammer weight or remodel the Proctor test. Second, as shown in Fig. 8, unlike the precise measuring system of the gyratory static compactor, the acceleration data used to build the impact compaction curve were quite scattered, which is partially due to the design of Marshall compactor. During the compaction, the hammer does not contact to the specimen directly but to a steel plate between them, which results in inevitable structural oscillations and noise. Future studies should design a laboratory compactor to avoid this and improve the data consistency. Third, as shown in Fig. 7, the actual impact compaction curve should be similar to the gyratory densification curve in Fig. 8 with a rising curve connected to a flat line. However, none trendlines including the three-order polynomial trendline could reflect this characteristic. More studies are needed to better describe the impact compaction curve. In future studies, various types of soil materials should be tested both in the laboratory and the field to establish the connection and the threshold for laboratory and field impact values.

6. Conclusions

Although new soil compaction technologies such as IC continue to emerge, the Proctor test for laboratory soil compaction has remained unchanged for decades. It is necessary to improve the laboratory compaction method to better understand the compaction process and the properties of soil for guiding the field compaction. In this study, a high-*g* accelerometer was installed on a laboratory impact compactor to monitor the compaction process of three types of aggregate and soils.

Based on the test results, the acceleration curve for each blow evolved to a stable pattern following the progress of compaction, and by identifying the occurrence of this pattern, the impact locking points for varying soils and moisture contents could be obtained, which had a similar trend to the gyratory locking points with R^2 equal to 0.59. By filtering the structural oscillations, the impact compaction curve could be constructed with the average acceleration value. Although each type of soil had a unique set of compaction curves, for the same soil, as the moisture content changed, the slope and value of compaction curve altered accordingly, which can be used to quantify the compactability of soil materials. Since a specific moisture content corresponds to a specific compaction curve for the same soil, a potential exists as using the compaction curve to predict the moisture content during the compaction. In addition, the average acceleration value of the final stage in the laboratory compaction could serve as the target value of soil stiffness. Therefore, besides the maximum dry density and optimum moisture content, the laboratory impact compaction has the potential to offer more parameters including locking point, compaction curve, and target stiffness of soil to guide the field compaction.

Declaration of competing interest

The authors declare that they have no known competing financial interests or personal relationships that could have appeared to influence the work reported in this paper.

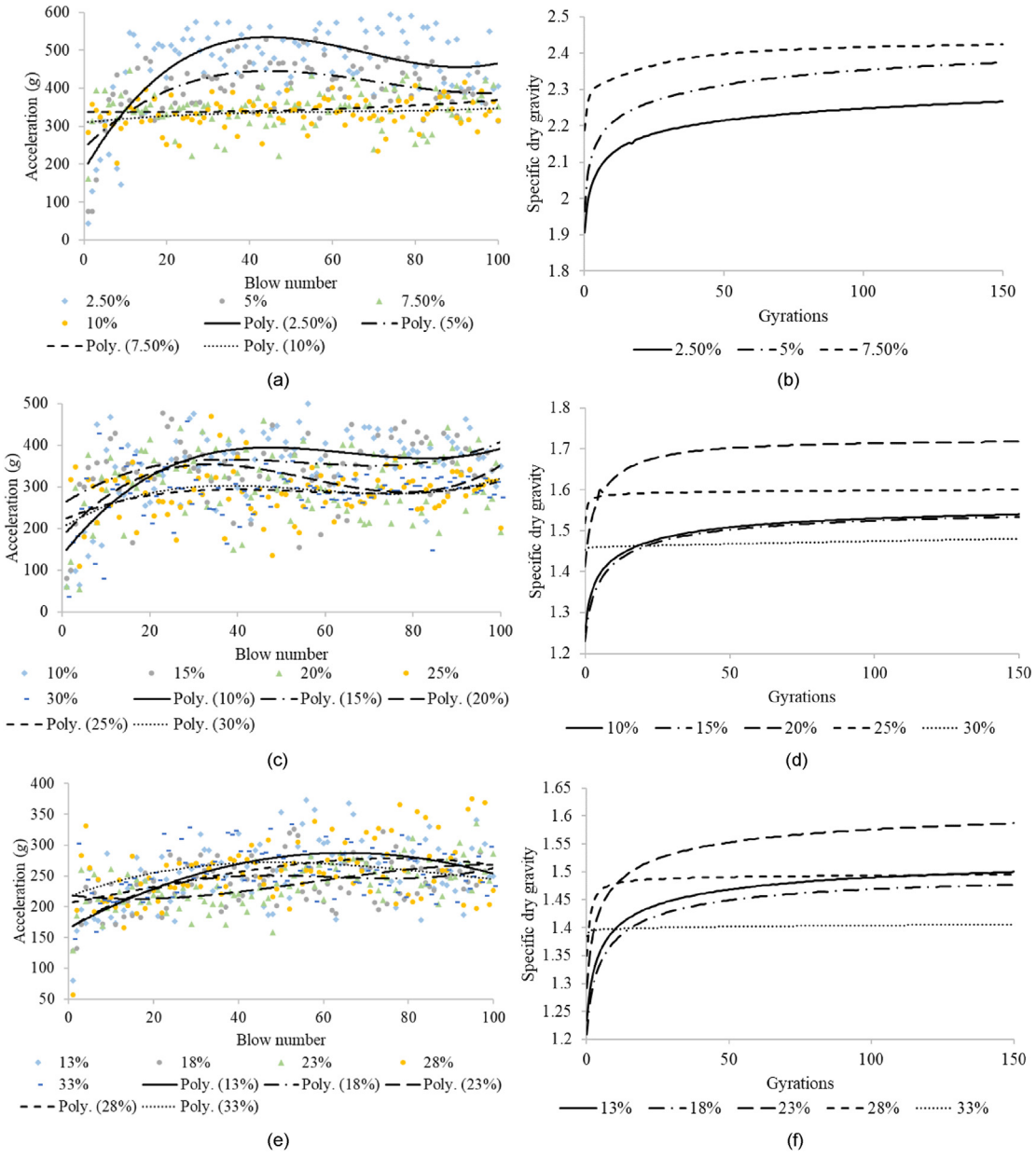

Fig. 8. Impact and gyratory compaction curves: (a) Aggregate impact compaction curve, (b) Aggregate gyratory compaction curve, (c) Soil 1 impact compaction curve, (d) Soil 1 gyratory compaction curve, (e) Soil 2 impact compaction curve, and (f) Soil 2 gyratory compaction curve. In the legend, the number in % represents the moisture content.

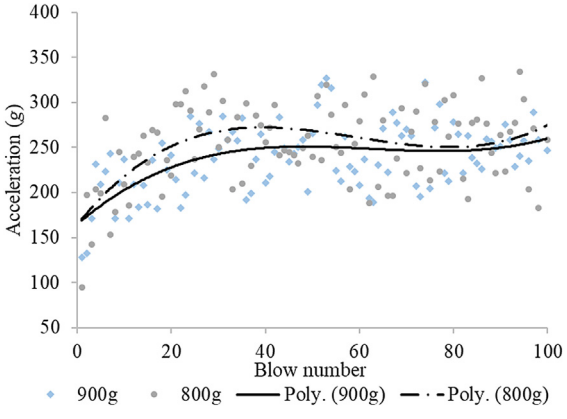

Fig. 9. Impact compaction curves with different sample masses.

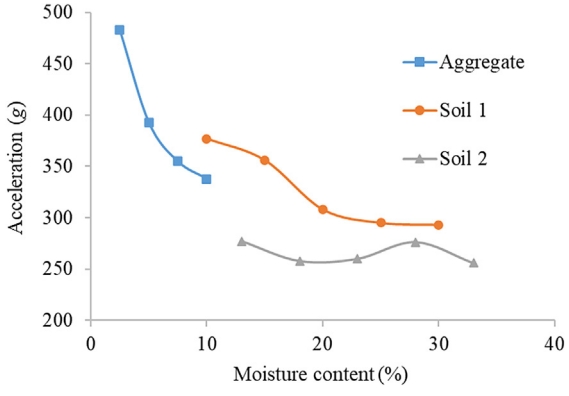

Fig. 10. Acceleration of the final stage vs. moisture content.

References

Anderson, R., Turner, P., Peterson, R., Mallick, R., 2002. Relationship of Superpave Gyratory Compaction Properties to HMA Rutting Behavior. NCHRP Report 478. Transportation Research Board, National Research Council, Washington, DC, USA.

Ba, M., Nokkaew, K., Fall, M., Tinjum, J.M., 2013. Effect of matric suction on resilient modulus of compacted aggregate base courses. Geotech. Geol. Eng. 31, 1497–1510.

Caicedo, B., Tristancho, J., Thorel, L., Leroueil, S., 2014. Experimental and analytical framework for modelling soil compaction. Eng. Geol. 175, 22–34.

Cetin, H., Fener, M., Söylemez, M., Günaydin, O., 2007. Soil structure changes during compaction of a cohesive soil. Eng. Geol. 92, 38–48.

Chow, Y., Yong, D., Yong, K., Lee, S., 1990. Monitoring of dynamic compaction by deceleration measurements. Comput. Geotech. 10, 189–209.

Clegg, B., 1976. An impact testing device for in situ base course evaluation. In: Proceedings of the Australian Road Research Board Conference.

Clegg, B., 1979. Application of an impact test to field evaluation of marginal base course materials. Transport. Res. Rec. 898, 174–181.

Das, B.M., Sobhan, K., 2013. Principles of Geotechnical Engineering. Cengage Learning.

Feng, S.-J., Tan, K., Shui, W.-H., Zhang, Y., 2013. Densification of desert sands by high energy dynamic compaction. Eng. Geol. 157, 48–54.

Hu, W., Jia, X., Zhu, X., Su, A., Du, Y., Huang, B., 2020. Influence of moisture content on intelligent soil compaction. Autom. ConStruct. 113, 103141.

Hu, W., Shu, X., Jia, X., Huang, B., 2017. Recommendations on intelligent compaction parameters for asphalt resurfacing quality evaluation. J. Construct. Eng. Manag. 143, 04017065.

Hu, W., Shu, X., Jia, X., Huang, B., 2018. Geostatistical analysis of intelligent compaction measurements for asphalt pavement compaction. Autom. ConStruct. 89, 162–169.

Ito, H., Komine, H., 2008. Dynamic compaction properties of bentonite-based materials. Eng. Geol. 98, 133–143.

Jia, X., Hu, W., Polaczyk, P., Gong, H., Huang, B., 2019. Comparative evaluation of compacting process for base materials using lab compaction methods. Transport. Res. Rec. 2673, 558–567.

Khan, Z.A., Wahab, H.I.A.-A., Asi, I., Ramadhan, R., 1998. Comparative study of asphalt concrete laboratory compaction methods to simulate field compaction. Construct. Build. Mater. 12, 373–384.

Kim, H., Prezzi, M., Salgado, R., 2010. Use of dynamic cone penetration and clegg hammer tests for quality control of roadway compaction and construction. In: Technical Report FHWA/IN/JTRP-2010/27. Purdue University, West Lafayette, USA.

Mohammad, L.N., Al-Shamsi, K., 2007. A look at the Bailey method and locking point concept in Superpave mixture design. In: Transportation Research Circular E-C124. Transportation Research Board. National Research Council, Washington, DC, USA, pp. 12–32.

Polaczyk, P., Han, B., Huang, B., Jia, X., Shu, X., 2018. Evaluation of the hot mix asphalt compactability utilizing the impact compaction method. Construct. Build. Mater. 187, 131–137.

Polaczyk, P., Huang, B., Shu, X., Gong, H., 2019a. Investigation into locking point of asphalt mixtures utilizing Superpave and Marshall compactors. J. Mater. Civ. Eng. 31, 04019188.

Polaczyk, P., Shu, X., Gong, H., Huang, B., 2019b. Influence of aggregates angularity on the locking point of asphalt mixtures. Road Mater. Pavement Des. 20, S183–S195.

Sebesta, S., Harris, P., Liu, W., 2008. Improving Lab Compaction Methods for Roadway Base Materia. In: Is. Technical Report FHWA/TX-07/0-5135-2. Texas Transportation Institute, Texas A & M University, College Station, TX, USA.

Shenton, H., Cassidy, M., Spellerberg, P., Savage, D., 1994. A system for calibration of the marshall compaction hammer. In: Technical Report FHWA-RD-94-002. Technical Analysis Division. National Institute of Standards and Technology, Gaithersburg, MD, USA.

Siddiqui, Z., Trethewey, M.W., Anderson, D.A., 1988. Variables affecting Marshall test results. Transport. Res. Rec. 1171, 139–148.

Vavrick, W., Huber, G., Pine, W., Bailey, R., 2002. Method summarized for gradation selection in hot-mix asphalt design. In: Transportation Research Circular E-C044. Transportation Research Board. National Research Council, Washington, DC, USA.

Vavrik, W., Carpenter, S., 1998. Calculating air voids at specified number of gyrations in Superpave gyratory compactor. Transport. Res. Rec. 1630, 117–125.

Virgil Ping, W., Yang, Z., Leonard, M., Putcha, S., 2002. Laboratory simulation of field compaction characteristics on sandy soils. Transport. Res. Rec. 1808, 84–95.

Vukadin, V., 2013. The improvement of the loosely deposited sands and silts with the rapid impact compaction technique on Brežice test sites. Eng. Geol. 160, 69–80.

Baoshan Huang obtained his BSc and MSc degrees in Civil Engineering at Tongji University, China, in 1984 and 1988, respectively, and his PhD in Civil Engineering at Louisiana State University, USA, in 2000. Currently, he is the Edwin G. Burdette Professor of Department of Civil and Environmental Engineering at the University of Tennessee, Knoxville (UTK) and the Director of Partnership for Sustainable Reuse of Solid Waste at UTK. He served as the Chair of American Society of Civil Engineers (ASCE) Bituminous Materials Committee (2010–2012), associate editors and editorial memberships for several reputable academic journals including the *Journal of Cleaner Production, ASCE Journal of Materials in Civil Engineering, ASCE Journal of Transportation Engineering Part B: Pavements, International Journal of Road Materials and Pavement Design, International Journal of Transportation Geotechnics*, etc. His areas of expertise include infrastructure materials and pavement engineering.